



Large Eddy Simulation of Turbulent Flows Around Two Canoe Paddles

Peter Parrish*, and Chunlei Liang †

Department Mechanical and Aerospace Engineering, Clarkson University, Potsdam, NY 13699

In this paper, a large-eddy simulation technique (LES) was used, incorporating a localized dynamic k -equation model (LDKM) to predict turbulent flows around two different canoe paddles. To assess the capability of the LDKM simulation technique, we analyzed flow past a square cylinder of finite height and compared against experimental results, achieving satisfactory accuracy in first- and second-order statistics. To further advance sporting technology, two popular canoe paddles used by US Northeast regional canoeing competitors were analyzed. To model a paddle stroke, a quasi-static approach was implemented, where analysis of the catching and power phases of the stroke cycle were performed. By evaluating flow structures, patterns, turbulence and quantifying blade propulsion, the LDKM model with wall functions demonstrated a strong potential for fine-tuning the designs of canoe paddle's blades. The high fidelity and robustness of LDKM in combination with a sophisticatedly calibrated mesh allow quantitative evaluation of the advantages of the curved-blade paddle for racing in the catching phase. To overcome the computational burden associated with LES, the simulations were run in parallel using 240 CPUs for each simulation.

Nomenclature

C_d	= coefficient of drag	d, h	= cylinder width and height
Re	= Reynolds number	w	= width of canoe paddle
τ'	= subgrid-scale stress tensor	C_p	= pressure coefficient
x, y, z	= dimensional spatial coordinates	A_p	= projected area of the paddle blade
X, Y, Z	= normalized spatial coordinates	t, T	= dimensional and normalized time
u, v, w	= dimensional velocity components	dt	= time step
U_∞	= fully developed stream-wise velocity	μ	= fluid viscosity
$\langle u \rangle$	= time averaged velocity components	ρ	= fluid density

I. Introduction

A. Background of Paddling Sports and Related Technology

In competitive canoe and kayak racing, advances in technology have proven to be a driving force in improving performance. Equipment design, material selection, and biomechanical optimization contribute significantly to speed and efficiency. A historical analysis of Olympic canoe and kayak events from 1948 to 2000 found several instances of technological breakthroughs that greatly affected race outcomes [1]. For example, improvements in kayak hull design greatly helped the United States achieve gold metals at the 1992 Olympics, and the Swedish winged paddle design is thought to have internationally increased performance times [1]. Continued research on improving canoe paddles has shown to improve paddling efficiency. Runciman et al. [2], have studied the negative effects of paddle resonance creating a mathematical model to quantify the fatigue that different paddles may induce. High-performance paddles often use carbon fiber composites to minimize these effects to facilitate greater force transmission during a stroke. For more in-depth coverage, the work of Shawn Burke [3] provides a fundamental examination of the sport of canoeing and

*Undergraduate Student, AIAA Student Member

†Professor, AIAA Associate Fellow

kayaking. Nolan and Bates [4], studied the effects of shaft bending and found that with a 15 degree bend angle between shaft and blade, a significant increase in performance can be expected.

One of the key questions regarding paddle design is the effect of the blade curvature. Despite extensive research on canoe and kayak hull design, comparatively fewer studies have investigated paddle optimization. Canoe paddles serve as the primary propulsion mechanism, making their geometry a critical factor in performance. Although both groups made significant contributions to paddle design, they do not cover the effects of blade curvature.

B. Prior Research on Canoe and Paddle Design

An earlier study by Plagenhoef examined the relationship between the athlete, the canoe, and the paddle [5], and idealized that the greater the distance in which the optimal force can be applied, the higher the achievable velocity. Re-shaping the paddle is certainly one way to accomplish this. Sumner et al. [6] made a good attempt not only to numerically model different canoe paddles but also to use experimental techniques using a water tunnel to further validate their arguments. However, their work did not take into account the curvature of the blade and rendered the paddles as flat plates. To get a complete picture of the fluid interactions, a complex 3D model would need to be used.

C. Large-Eddy Simulation Overview

Large-Eddy Simulation (LES) is a computational fluid dynamics (CFD) technique used to model turbulent flows by explicitly resolving large-scale turbulent structures while modeling the effects of smaller sub-grid-scale eddies using either implicit (kinetic energy dissipation implied numerically) or explicit (through the use of a modeled sub-grid). LES was developed as a middle ground between direct numerical simulation (DNS), which resolves all the turbulence scales at immense computational cost, and Reynolds-average Navier-Stokes (RANS) models, which rely entirely on statistical turbulence closure. First introduced by Smagorinsky in 1963 for atmospheric turbulence modeling [7], LES has since become a key method in fluid engineering applications involving unsteady flows of high Reynolds number, such as aerodynamics, combustion, and hydrodynamics. Compared to RANS, LES provides a higher level of accuracy in transient flow predictions, which makes it particularly valuable for studying complex engineering problems and is essential for studying the time-dependent interactions between the paddle and its surrounding fluid.

Among various LES subgrid-scale models, the local dynamic K-Equation model provides an adaptive approach to turbulence modeling by dynamically adjusting the turbulence energy equation at each time step. Based on the dynamic modeling framework designed by Germano et al. [8], the LDKM model adapts to varying flow conditions, making it particularly suitable for simulations in which local flow structures change significantly over time.

This LES-LDKM method is implemented using OpenFOAM, an open source CFD software widely used for its simulation capabilities. The software allows for the customization of turbulence models and grid structure and refinement. However, OpenFOAM has limitations, including a steep learning curve and a high cost in computational resources. Monroe's work [9] validated comparable simulation approaches for marine water jet flows with Reynolds numbers greater than 4 million. For a detailed discussion of these validation methods, readers are referred to Monroe's study.

D. Motivation and Objectives

The motivation for this study comes from discussions with GRB Newman Designs, a canoe and paddle manufacturer that specializes in high-performance paddling equipment. Their design philosophy suggests that the blade curvature may provide advantages over a straight design by improving the water catch efficiency. Specifically, they propose that a curved-blade paddle aligns better with the water in the catching phase, minimizing downward force losses. During the power phase, the performance difference is expected to be minimal, as fluid resistance depends primarily on the projected surface area rather than the blade curvature. However, in the exit phase, the curved blade can pose a more challenging exit, but for both blade designs, a fast withdrawal away from the canoe is preferred. Due to this fast blade removal, the quasistatic approach implemented in this paper will not factor into the exit phase as it does not contribute to the overall propulsion of the craft. Although these ideas align with fundamental fluid mechanics, a rigorous numerical evaluation is necessary to validate these claims and quantify their effects.

This method can potentially quantify the difference in flow control between curved and straight-blade canoe paddles, evaluating their potential advantages and disadvantages in key stroke phases. To achieve this, novel Large Eddy Simulation (LES) techniques are implemented using the Local Dynamic K-Equation (LDKM) model, providing a high-fidelity computational approach for a precise understanding of paddle optimization for competitive canoe sports. This paper also aims to demonstrate the capabilities of LES in this simple but complex engineering application.

II. Computational model

A. Problem description

The objects in Figure 2 are 3D CAD models created by scanning each paddle using Clarkson's Li-DAR scanning techniques. There is a 12-degree bend between the blade and the shaft for both straight-blade and curved-blade paddles; however, the curved-blade paddle also has a 12-degree bend at its tip.

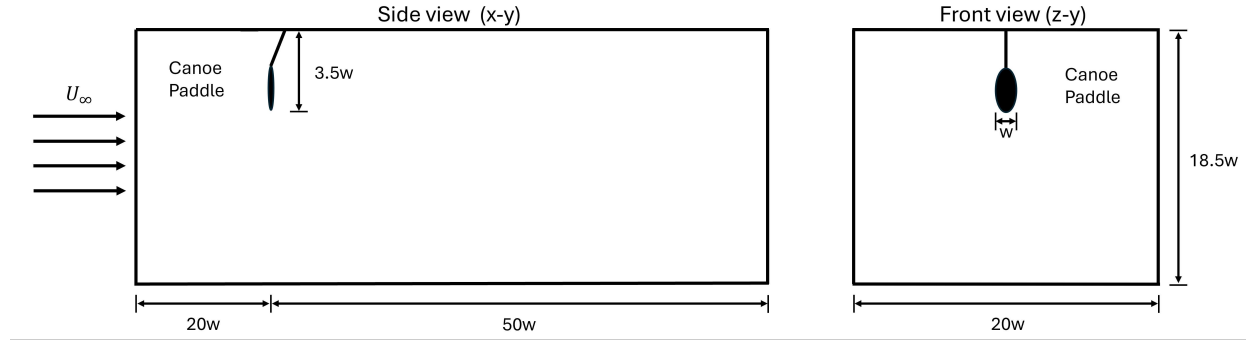


Fig. 1 Computational domain of the canoe paddle setup

In Figure 1, a computational domain is chosen to study the flow past a canoe paddle. The width of the paddle (w) is 0.2 m. The paddle is placed 25 w downstream of the inlet and 50 w upstream of the outlet. To ensure that the domain has minimal blockage effects on paddle characteristics, a depth of 23 w is used. A uniform velocity profile and pressure outlet are provided at the inlet and outlet boundaries, respectively. To keep the Reynolds number of 200,000 for the flow, the inlet velocity was set at 1 m/s. A synthetic turbulence generator algorithm is used as a fluctuating velocity at the input. The turbulent intensity and turbulent viscosity ratio are 5% and 10 respectively applied at the inlet velocity. For this problem, a stationary non-slip wall was used on the paddle and shaft. The boundary condition of the free surface and all other surfaces of the domain are modeled with the boundary condition of the zero velocity gradient. A similar approach was consistently adopted in 4 different geometric setups to evaluate flow fields around both curve and straight-blade paddles with two different angles of attack.

B. Large eddy simulation

The local dynamic k-equation model (LDKM) proposed by Kim and Menon [10] is more computationally demanding than most and, because of this, is more expensive to use. Although it is more expensive, it is desirable due to its time-accurate and higher-fidelity nature. Much like other CFD solvers, conservation of mass and momentum equations is applied, but unlike others, a low-pass filter uses information from the grid to generate a sub-grid eddy model. This allowed eddies that were too small to be picked up by the mesh to be modeled.

The filtered continuity and momentum equations for incompressible flow are given by:

$$\frac{\partial(\rho \tilde{u}_j)}{\partial x_j} = 0 \quad (1)$$

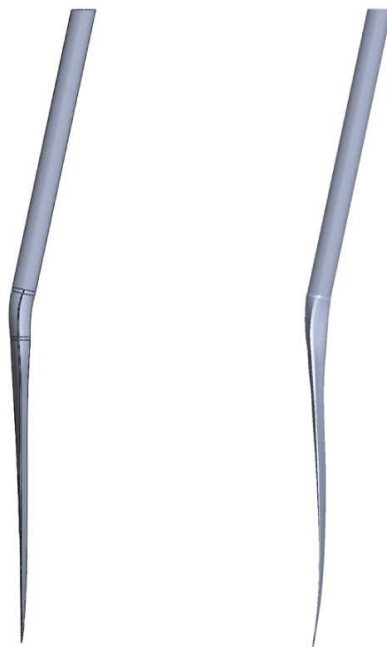


Fig. 2 Modeled geometry of GRB's straight (left) and curved (right) blade paddles in a side by side configuration.

$$\frac{\partial(\rho\tilde{u}i)}{\partial t} + \frac{\partial(\rho\tilde{u}i\tilde{u}j)}{\partial x_j} = -\frac{\partial(\tilde{p}\delta_{ij})}{\partial x_j} + \frac{\partial\tau'_{ij}}{\partial x_j} + 2\mu\frac{\partial\tilde{s}_{ij}}{\partial x_j} \quad (2)$$

where \tilde{s}_{ij} is the filtered strain rate tensor, and the stress tensor of the subgrid scale (SGS) is defined as:

$$\tau'_{ij} = \rho\tilde{u}_i\tilde{u}_j - \rho\tilde{u}_i\tilde{u}_j \quad (3)$$

The transport equation for the kinetic energy on the subgrid scale, k_{sgs} , is given by:

$$\frac{\partial k_{sgs}}{\partial t} + \tilde{u}_i \frac{\partial k_{sgs}}{\partial x_i} = -\tau_{ij} \frac{\partial \tilde{u}i}{\partial x_j} - \varepsilon_{sgs} + \frac{\partial}{\partial x_i} \left(\nu_T \frac{\partial k_{sgs}}{\partial x_i} \right) \quad (4)$$

where the terms on the right-hand side represent, respectively, the production, dissipation, and transport of kinetic energy on the subgrid scale. These quantities are expressed as follows.

$$k_{sgs} = \frac{1}{2} \left(\overline{u_k^2} - \tilde{u}_k^2 \right) \quad (5)$$

$$\varepsilon_{sgs} = C_\epsilon \frac{k_{sgs}^{3/2}}{\bar{\Delta}} \quad (6)$$

$$\nu_T = C_\nu \bar{\Delta} k_{sgs}^{1/2} \quad (7)$$

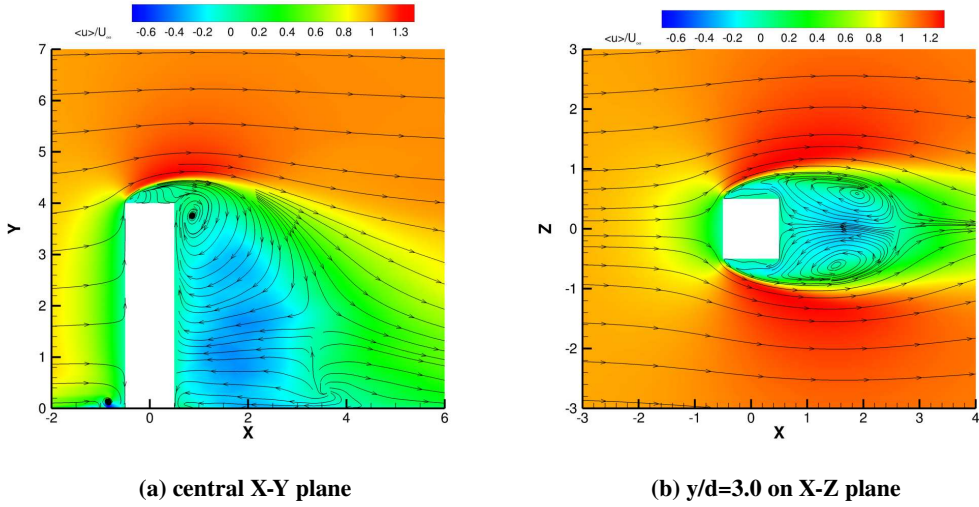
where C_ϵ and C_ν are model coefficients determined from local flow properties.

C. Validation

To validate this model, the case of a square cylinder is used. The experimental and numerical data reported by Saeedi and Wang [11] are compared to the results of the large-eddy simulations obtained in this study. It should also be mentioned that the experimental work done by Bourgeois et al. [12] has greatly contributed to the validation of this case. Through the use of a wind tunnel, they were able to gather the data used to validate the model used here.

The square cylinder is simulated at a Reynolds number of nearly 12,000. This study is carried out using a different LES model (LDKM) compared to the computational results and experimental data reported in the work of Saeedi and Wang (2016) [11], which used a dynamic Smagorinsky approach. The computational domain is discretized with the use of openFOAM's SnappyHexMesh. The Filtered governing equations are discretized using the finite-volume method with unstructured grid formatting. For pressure and velocity coupling, a PIMPLE algorithm is used. Periodic boundary conditions are applied in the spanwise direction. The standard no-slip boundary condition is used for the cylinder wall. The wall functions 'nutUsplandWallFunction' and 'kqRwallFunction' are added to the LDKM model of the near-wall dynamics for all cases in this paper.

Figure 3 (a) shows the average time contour in the stream velocity in the center of the xy plane. The model is able to capture the vortex generated near the downstream and flow separation at the top of the cylinder wall. In Figure 3 (b), a time-averaged streamwise velocity contour is presented at an elevation of $y/d=3$ over the x-z plane. It has been observed that flow separation is created at the edge of two sides and two symmetrical vortex is created on both sides. These contour results are similar to the results observed in the Saeedi and Wang paper. The quantitative results of the streamwise and spanwise time-averaged velocities over time are shown in Figure 4.

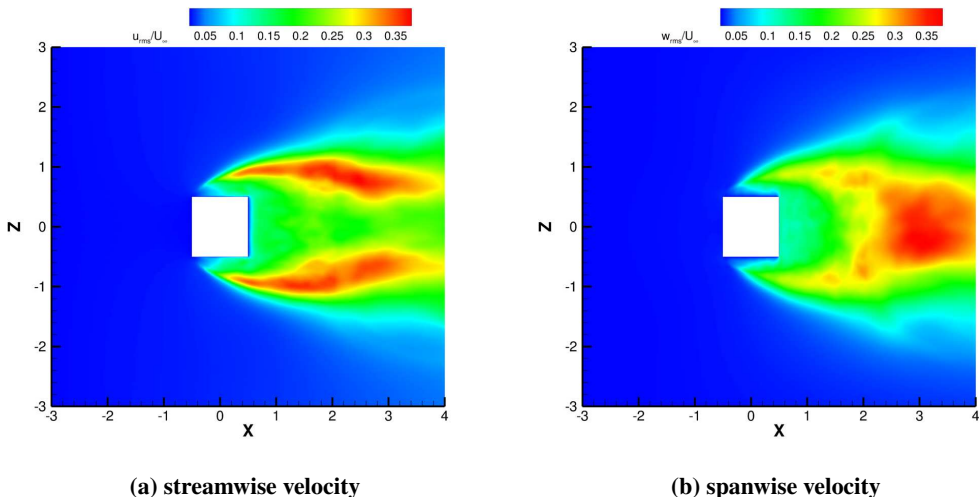


(a) central X-Y plane

(b) $y/d=3.0$ on X-Z plane

Fig. 3 Non-dimensionalized time average stream-wise velocity contours.

The normalized RMS velocity contours along the streamwise and spanwise directions are shown in Figure 5 in the xz plane. In Figure 5 (a), the streamwise turbulence fluctuations on the left and right sides of the cylinder are due to the generation of vortex, as shown in Figure 3 (b). The quantitative variation of streamwise RMS velocity in the vicinity ($x/d = 2$) and away ($x/w = 3.5$) from the cylinder is shown in Figure 6 (a) and (b). The RMS velocity is higher on two sides of the cylinder because two vortices are generated on two sides of the cylinder. In 5 (b) the spanwise velocity fluctuation is more at the downstream center location after the vortex generation is complete. The quantitative results are shown in Figures 6 (c) and (d) agree with those results reported in the article by Saeedi and Wang [11]. However, a similar trend and the general magnitudes of the velocity profiles are observed in this study in accordance with the work of Saeedi and Wang [11].



(a) streamwise velocity

(b) spanwise velocity

Fig. 5 RMS velocity contours at $y/d=3$ on xz plane.

The isometric view of the results of the non-dimensional pressure fluctuation of -0.2 is shown in Figure 7 (a). The Q criterion for flow past a square cylinder is shown in 7 (b). Using the Q criterion, we are able to capture smaller vortices nearer to the cylinder.

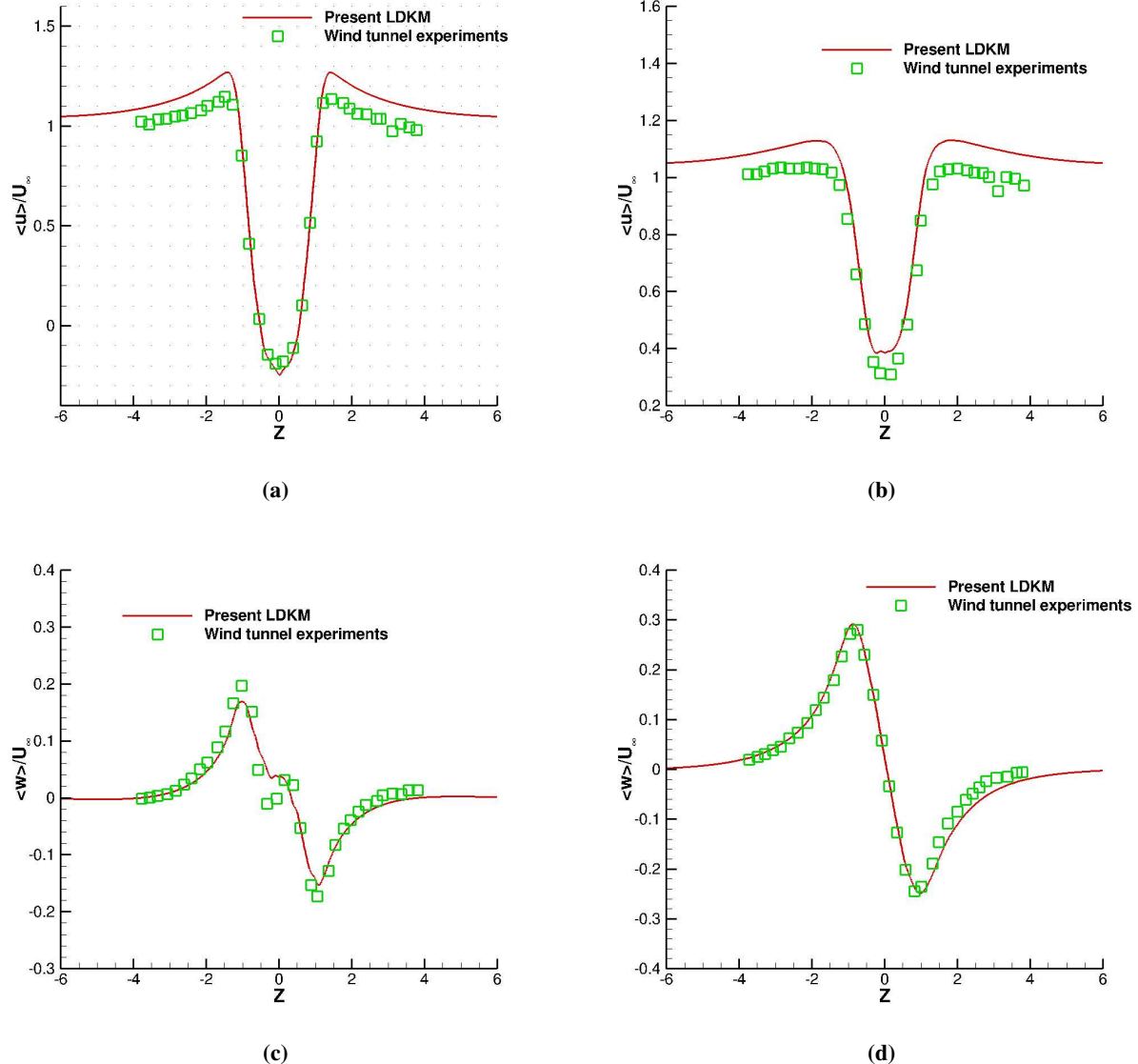


Fig. 4 Time-averaged streamwise velocity at (a) $x/d=2$, (b) $x/d=3.5$ and time-averaged spanwise velocity (c) $x/d=2$, (d) $x/d=3.5$ at plane $y/d=3$.

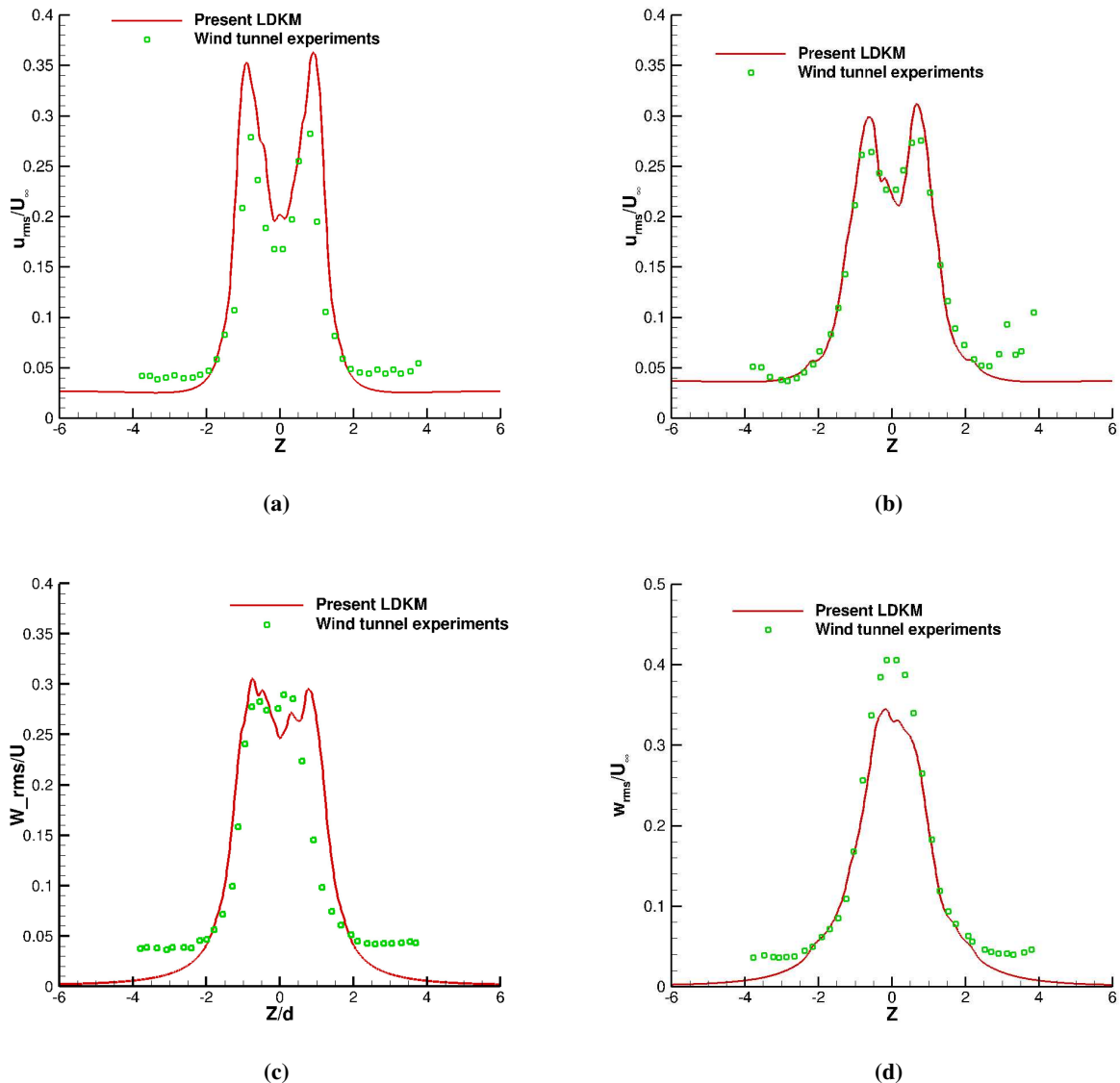


Fig. 6 Streamwise RMS velocity at (a) $x/d=2$, (b) $x/d=3.5$ and spanwise RMS velocity at (c) $x/d=2$, (d) $x/d=3.5$ at plane $y/d=3$.

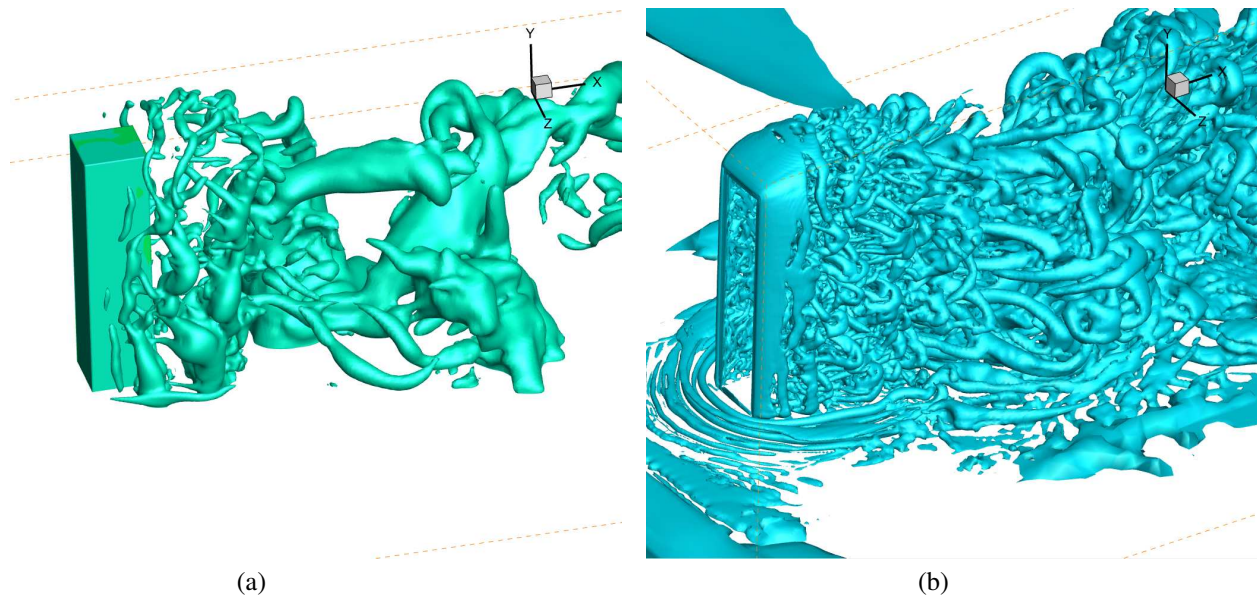


Fig. 7 Isosurface (a) non-dimensional p' ($p' = -0.2$) (b) non-dimensional Q value ($Q = 0.00035$).

D. Numerical implementation

The numerical simulation of the two canoe paddles was performed using a similar LES technique as demonstrated by Monroe [9]. This model was adopted because of the large flow separation and the high Reynolds number of this case, generating a significant amount of small eddies that are not able to be graphed by the larger grid. The LDKM overtechnical is used to resolve these smaller eddies. The grid size used in these simulations contained close to 7.8 million elements. Although the geometry differed, the surface areas remained the same, making each mesh relatively similar with a difference of only 1000 cells. In Figure 8 the "blade mesh" shows the snappyHexMeshes ability to capture the surface of the geometries reasonably well, with a fairly coarse element size of 1mm. At parts where the blade thickness approaches 1mm the mesh generates surface features preventing the mesh from failing but at the same time sacrificing accuracy. The *min refinement zone*, contains cells of 16mm in length. Several layers of buffer were added to help reduce interpolation errors between cell sizes.

Due to the high velocity around the canoe paddle, wall modeling becomes necessary to capture the smaller eddies interfacing directly with the oncoming fluid. The momentum equation is discretized by a bounded central difference scheme where the pressure terms are of the second order. Bounded second-order implicit is implemented for the transient terms in the equations to mention stability and accuracy. For pressure velocity coupling, a PIMPLE scheme is used. During this simulation, the convergence criterion is 10^{-6} . The time marching during these simulations was set to 0.003 s with no more than 30 sub-iterations, although most time steps converged within 6 iterations. In order to compute parallelization of the domain, 240 processors are used. The computational domain has been discretized using 7.6 million unstructured cells. In future studies, it will be required to refine the mesh to produce a well-captured flow; however, for the purposes of this paper, the flow relied heavily on wall modeling to produce well-resolved near-wall dynamics.

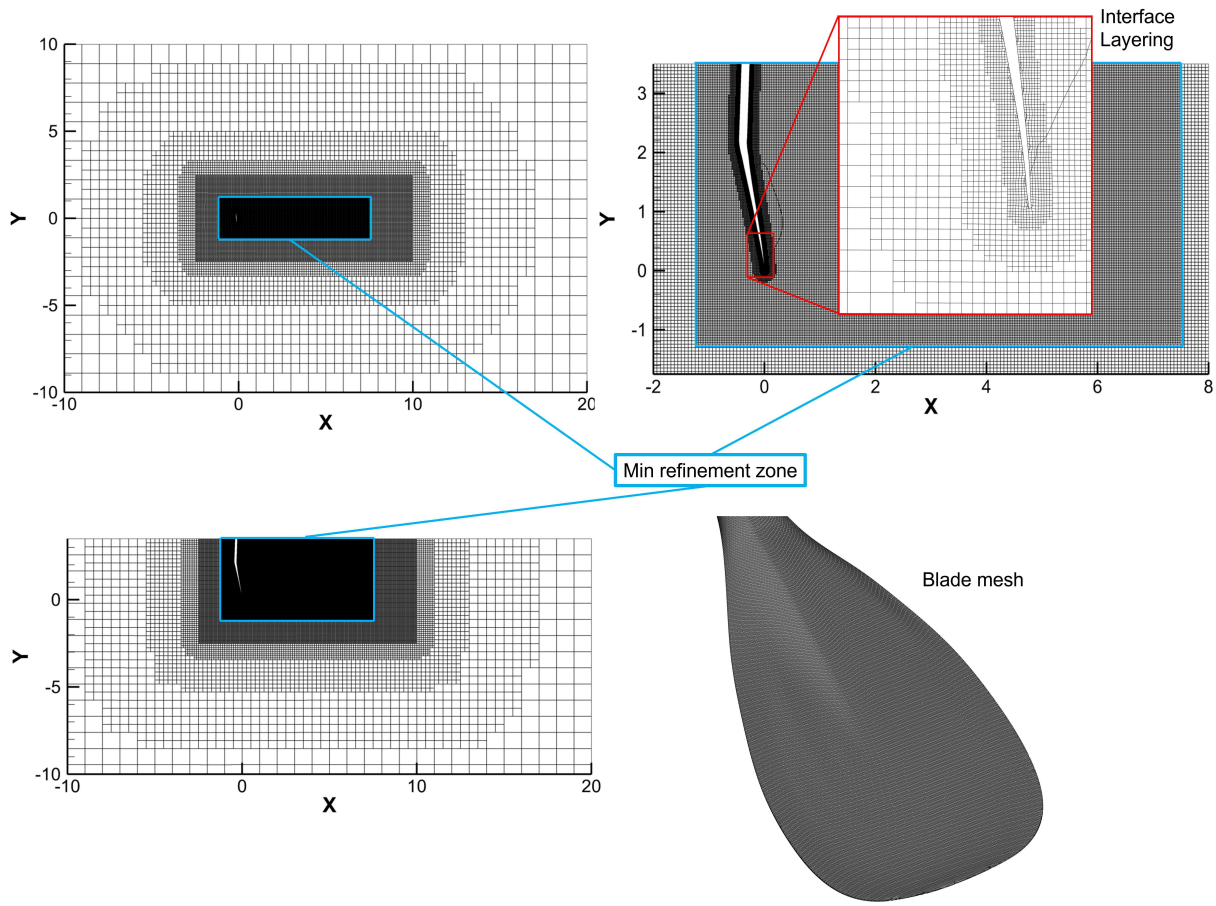


Fig. 8 Paddle and domain mesh discretization

III. Results and discussions

A. Time History

The hydrodynamic pressure acting on a canoe paddle during a stroke is primarily composed of pressure and viscous forces. Understanding their time-dependent behavior provides insight into paddle efficiency, fluid interactions, and propulsion mechanics. This section examines the time history of these forces in the collected results. In future studies, it may be important to increase the amount of time simulated to produce statistically stabilized results. However, for this study, reasonable results were obtained after 15 seconds of simulation. To reduce the effects of instability, the first 4 seconds of all the results in the study were removed. The preliminary time history is presented in Figure 9.

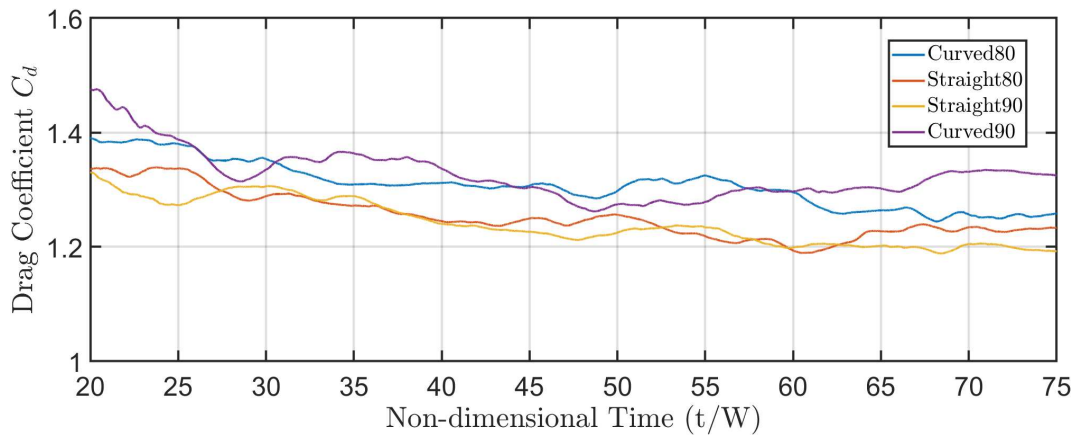


Fig. 9 Time history of pressure and viscous forces

B. Flow Structures and Characteristics

The analysis of flow structures and characteristics was performed to assess the performance of this method in a real-world design application. These initial flow behaviors and observations revealed distinct structural formations related to the tips of the canoe paddles, as well as the relative positions of their respective recirculation bubbles. The visualization of the flow structures as seen in Figure 10 showed coherent patterns with three evident recirculation bubbles for both designs. The top vortex that recirculates along the clockwise direction is formed from the blade shoulders with respect to the shaft. It is also clear that the curved-blade paddle has recirculation closer to the blade wall.

Further investigation of the geometry in the catching phase of the stroke reveals that along the tips of the blades, both paddles generate large tip vortices recirculating along the counterclockwise direction. As seen in Figure 10, the lower and tighter recirculation at the tip is located near the blade. This vortex travels over the length of the tip, translating a significant amount of power from the paddler to the water. The pressure contours in Figure 10 clearly prove that the curved-blade paddle has higher drag. However, in this paper, no graphics on the X-Z planes are shown for 3D views of the recirculation bubbles, and the increase in propulsive performance is nevertheless reflected in the time history shown in Figure 9.

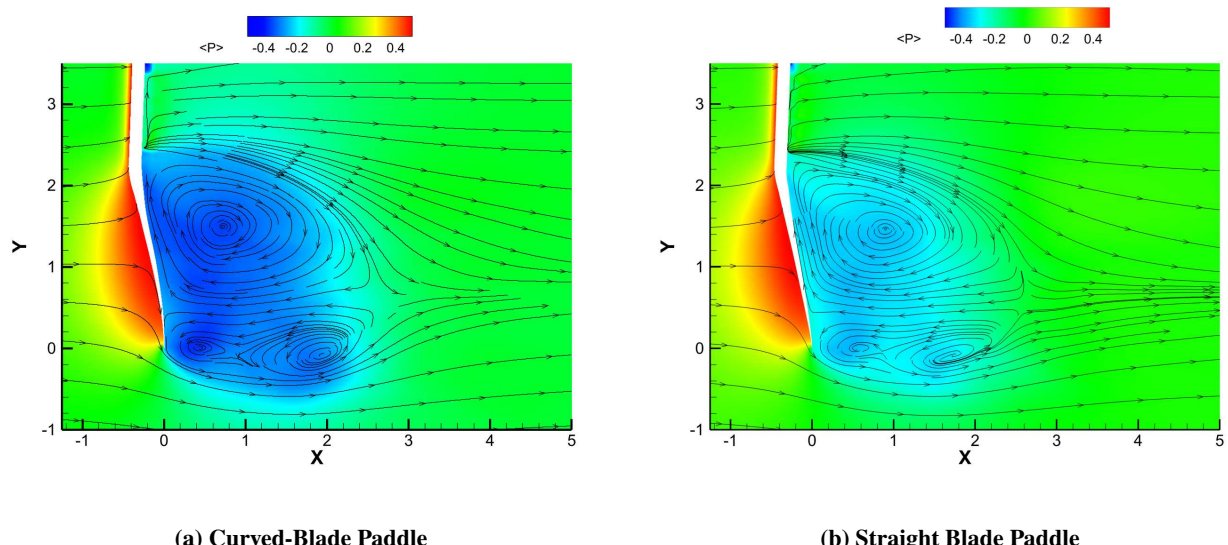


Fig. 10 Mean pressure contours in the central X-Y plane with streamlines for both paddle configurations.

IV. Concluding Remarks

In general, the flows around canoe paddles exhibit intense turbulence that can be modeled with the use of a high-fidelity explicit large-eddy simulation technique. This study demonstrates the effectiveness of the LDKM model in capturing complex flow structures and turbulence characteristics around the paddle during the catching phase. This subgrid-scale model is used in combination with two wall functions, as well as a nested grid refinement feature of snappyHexMesh works well to improve numerical accuracy for near-wall wake dynamics. The curved-blade paddle, while maintaining roughly the same surface area as the straight-blade paddle, is able to offer more drag and thus more propulsion during the catching phase of the paddle stroke cycle. This suggests that the geometry of the paddle blades plays a crucial role in optimizing hydrodynamic performance. The GRB Newman Designs curved-blade paddle generates a greater propulsive force in the catching phase due to the lower pressure concentration behind the blade. These findings contribute to a better understanding of paddle hydrodynamics and could inform future design optimizations to improve efficiency in canoeing.

Acknowledgments

The authors acknowledge support from Clarkson University and the Department of Mechanical and Aerospace Engineering. Our computations were performed on Clarkson's ACRES cluster. The first author thanks research discussions with Dr. Aurabinda Swain and Ph.D. student Ibrahim Fetuga from Professor Liang's group.

References

- [1] Robinson, M. G., Holt, L. E., and Pelham, T. W., "The Technology of Sprint Racing Canoe and Kayak Hull and Paddle Designs," *International Sports Journal*, Vol. 6, 2002, pp. 68–85.
- [2] Runciman, R. J., Lyle, K., and Patrick, L., "Canoe paddle resonance characteristics and modelling," *Journal of Sports Engineering and Technology*, Vol. 226, 2012, pp. 42–51.
- [3] Burke, S., *The Science of Paddling*, Welos Book Works, 2023.
- [4] Nolan, G. N., and Bates, B. T., "A Biomechanical Analysis of the Effects of Two Paddle Types On Performance in North American Canoe Racing," *Research Quarterly for Exercise and Sport*, Vol. 53, 1982, pp. 50–57.
- [5] Pleggenhoef, S., "Biomechanical Analysis of Olympic Flatwater Kayaking and Canoeing," *Research Quarterly. American Alliance for Health, Physical Education, Recreation and Dance*, Vol. 50, 1979, pp. 443–459.
- [6] Sumner, D., Sprigings, E., Bugg, J., and Heseltine, J., "Fluid forces on kayak paddle blades of different design," *Sports Engineering*, Vol. 6, 2003, pp. 11–19.
- [7] Smagorinsky, J., "General circulation experiments with the primitive equations: I. The basic experiment," *Monthly weather review*, Vol. 91, No. 3, 1963, pp. 99–164.
- [8] Germano, M., Piomelli, U., Moin, P., and Cabot, W. H., "A dynamic subgrid-scale eddy viscosity model," *Physics of Fluids A: Fluid Dynamics*, Vol. 3, No. 7, 1991, pp. 1760–1765.
- [9] Monroe, S., "URANS and LES Studies of Turbulent Flows in an ONR Waterjet Pump using Unstructured Grids with Sliding Mesh Interfaces," Master's thesis, Clarkson University, 2024.
- [10] Kim, W.-W., and Menon, S., "A new dynamic one-equation subgrid-scale model for large eddy simulations," *33rd aerospace sciences meeting and exhibit*, 1995, p. 356.
- [11] Saeedi, M., and Wang, B. C., "Large-Eddy Simulation of Turbulent Flow Around a Finite-Height Wall-Mounted Square Cylinder Within a Thin Boundary Layer," *Flow Turbulence Combust*, Vol. 97, 2016, p. 513–538.
- [12] Bourgeois, J. A., Sattari, P., and Martinuzzi, R. J., "Alternating half-loop shedding in the turbulent wake of a finite surface-mounted square cylinder with a thin boundary layer," *Physics of Fluids*, Vol. 23, 2011, pp. 95101–95116.